

Timing Signatures of the Internal-Shock Model for Blazars

Markus Boettcher (Ohio University), Charles D. Dermer (NRL)

Abstract: We have developed a semi-analytical model for the time-dependent radiative output from the internal-shock model for blazars. Accounting for spatial inhomogeneities due to the forward- and reverse-shock propagation and light travel time effects, the synchrotron and external-Compton emissions are evaluated completely analytically, while the synchrotron self-Compton emission is reduced to a two-dimensional integral. We explore the influence of various parameters on the time-averaged spectral energy distributions and timing features for parameters suitable for flat-spectrum radio quasars and low-frequency peaked BL Lac objects. Light curves at various representative photon energies are subjected to the Discrete Correlation Function to evaluate inter-band time lags, as is routinely done for observational data.

Model Setup: Figure 1 illustrates the geometry of our model: Two shells of initially cold (i.e., internal energy \ll bulk kinetic energy) plasma with Lorentz factors Γ_a and Γ_b ($\Gamma_b > \Gamma_a \gg 1$) collide, leading to a forward shock propagating into shell a and a reverse shock propagating into shell b.

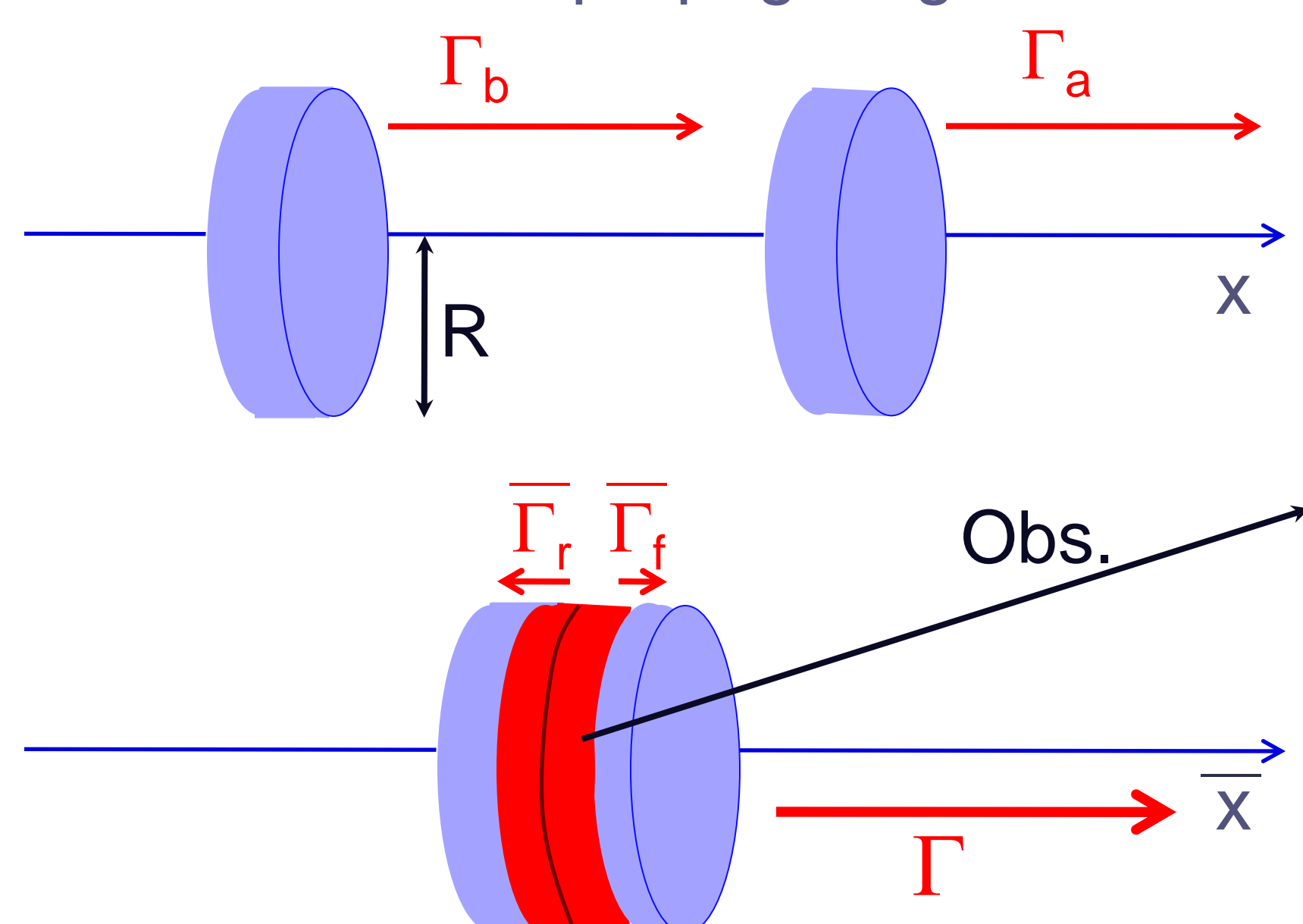


Fig. 1: Geometry of the shell collision leading to internal shocks in a blazar jet.

The shocked fluid will move with Lorentz factor Γ with respect to the stationary frame. In the frame comoving with the shocked fluids, the shocks propagate with Lorentz factors $\bar{\Gamma}_f$ and $\bar{\Gamma}_r$, respectively.

Particle Dynamics: At the shocks, particles are assumed to be accelerated into a power-law distribution with index q , with normalization and low- and high-energy cutoffs determined by energy conservation and balancing of acceleration and radiative cooling time scales. Subsequent radiative cooling is taken into account assuming synchrotron + Compton cooling in the Thomson regime, leading to a fully analytical space- and time-dependent electron energy distribution throughout the shocked region.

Radiation: Synchrotron and external-Compton emission is evaluated analytically using a δ -function approximation. The space- and time-dependent synchrotron photon density is also evaluated analytically and used for a numerical computation of the space- and time-dependent SSC emissivity. All time delays from shock- and light-travel time effects are properly taken into account.

Baseline Model: For a baseline model, we use parameters reproducing a Spectral Energy Distribution (SED) typical of Flat Spectrum Radio Quasars (FSRQ) or Low-frequency peaked BL Lac Objects (LBL), as listed in the table.

These parameters lead to a bulk Lorentz factor of the shocked fluid of $\Gamma = 18.2$, and we choose the observing angle so that the Doppler factor $D = \Gamma = 18.2$.

Parameter	Symbol	Value
Lorentz Factor of shell a	Γ_a	15
Lorentz Factor of shell b	Γ_b	25
Kinetic power of shell a	L_a	10^{47} erg/s
Kinetic power of shell b	L_b	10^{47} erg/s
Time scale for ejection of shells	Δt	10^3 s
Electron equipartition fraction	ϵ_e	0.2
Magnetic-field equipartition fraction	ϵ_B	10^{-3}
Electron injection spectral index	q	2.3
External radiation energy density	u_{ext}	10^{-4} erg/cm ³
External radiation peak frequency	ν_{ext}	$3 \cdot 10^{14}$ Hz
Cross-sectional radius of shells	R	$3 \cdot 10^{15}$ cm
Redshift	z	0.2

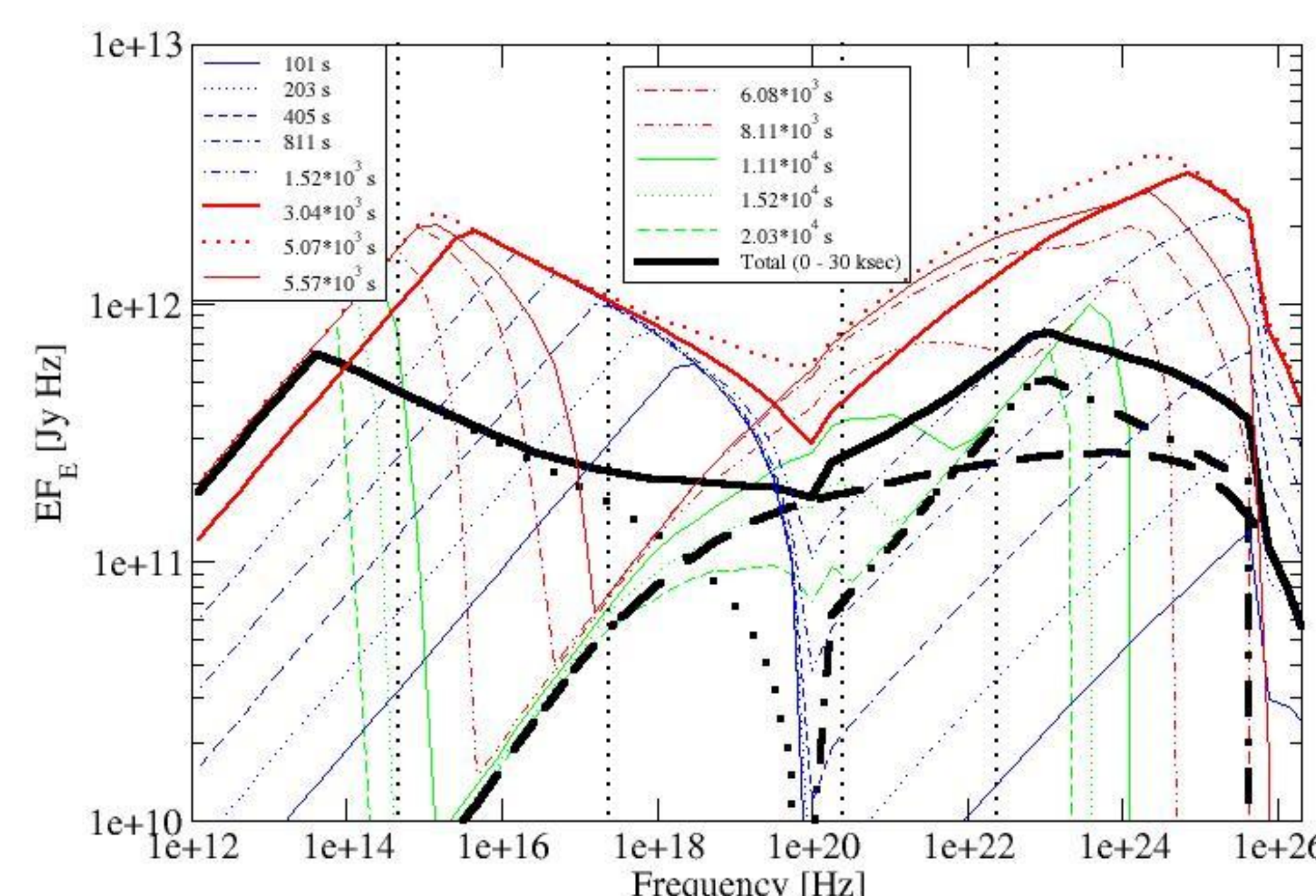


Fig. 2: Snap-shot SEDs from our baseline model, along with the SED time-averaged over 30 ksec (heavy black curves). Dotted vertical lines indicate the frequencies at which light curves have been extracted.

In addition to snap-shot SEDs, we calculate the time-averaged spectrum over an integration time of 30 ksec to investigate averaged SED characteristics.

Light curves have been extracted at four frequencies: Optical (**R-band**), X-rays (**1 keV**), soft γ -rays (**1 MeV**), and high-energy γ -rays in the Fermi range (**100 MeV**). Cross-correlations and time lags between the light curves have been investigated using the **Discrete Correlation Function** (DCF; Edelson & Krolik 1988).

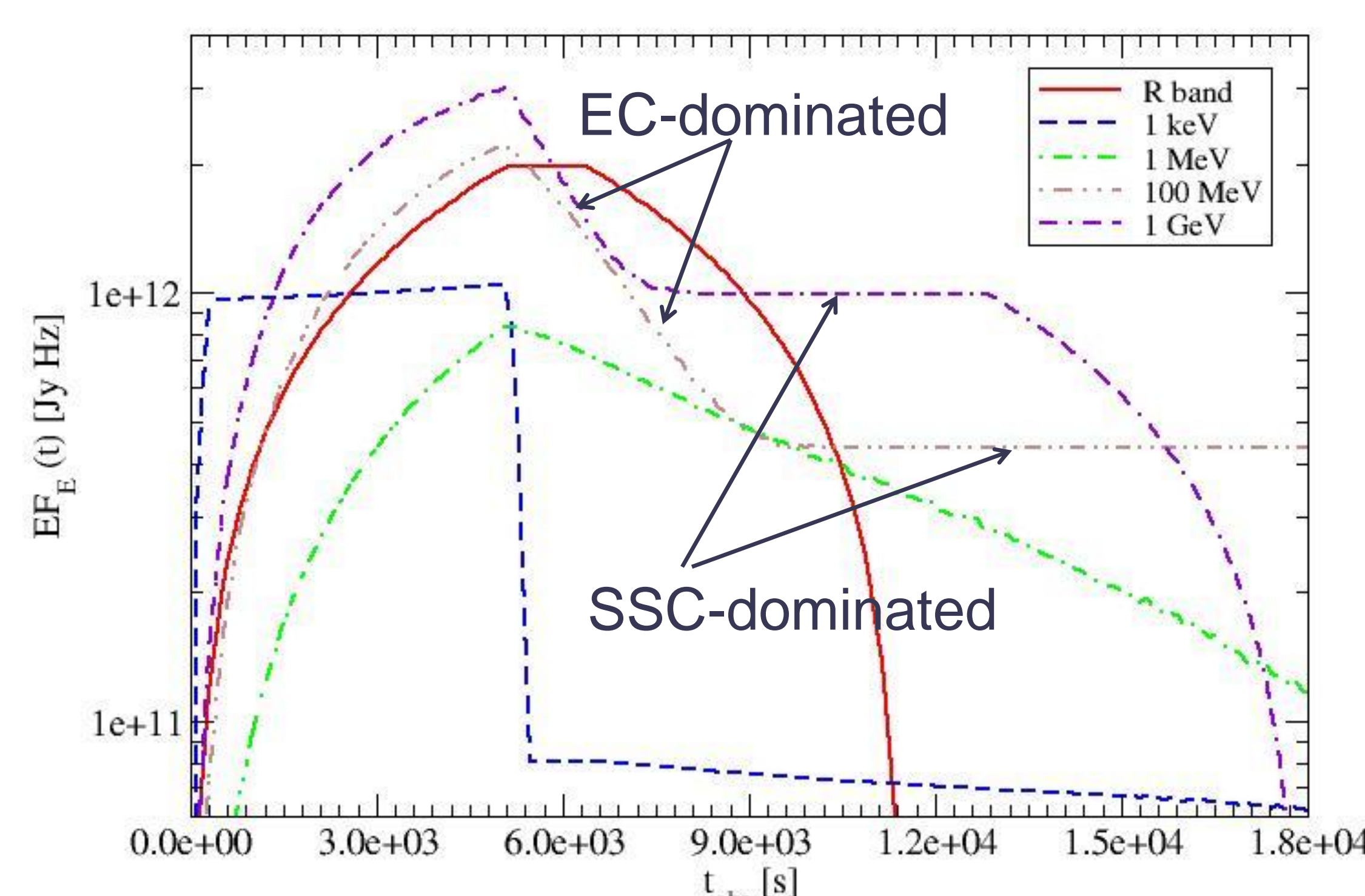


Fig. 3: Light curves resulting from our baseline model

Figure 4 illustrates the DCF results for our baseline model: It predicts lags of the R-band and soft γ -rays behind soft X-rays by $\sim 1 - 2$ hrs with sub-hr time lags between other bands.

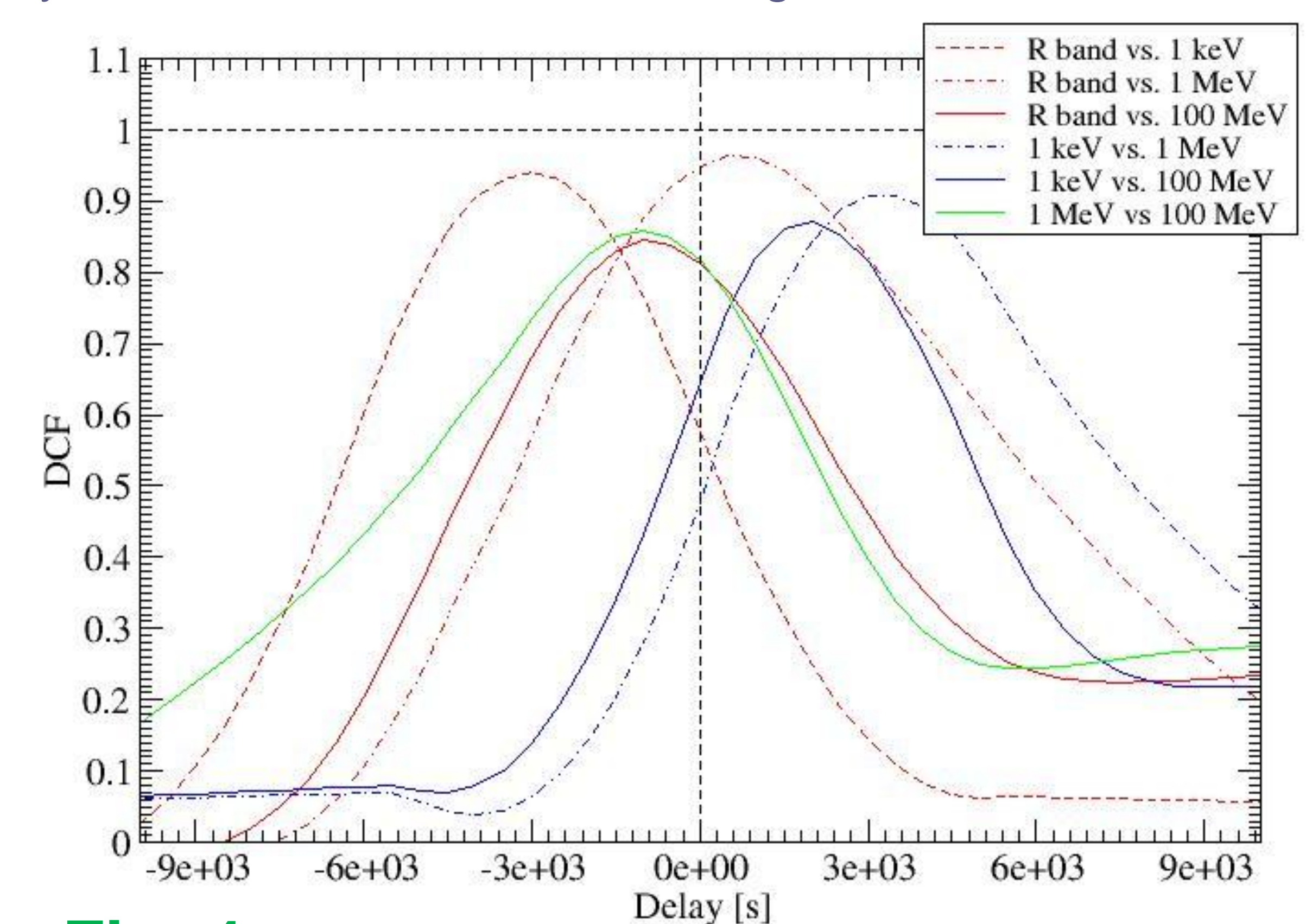


Fig. 4: Discrete Correlation Functions (DCFs) between light curves from our baseline model.

The dependence of these features on various parameters has been investigated. As an example, Fig. 5 illustrates the dependence of DCF characteristics on the external radiation field. Most notably, this and other parameter variations may lead to a **change in sign of time lags**, e.g., a transition from an R-band lag behind HE γ -rays to an R-band lead with increasing external radiation energy density.

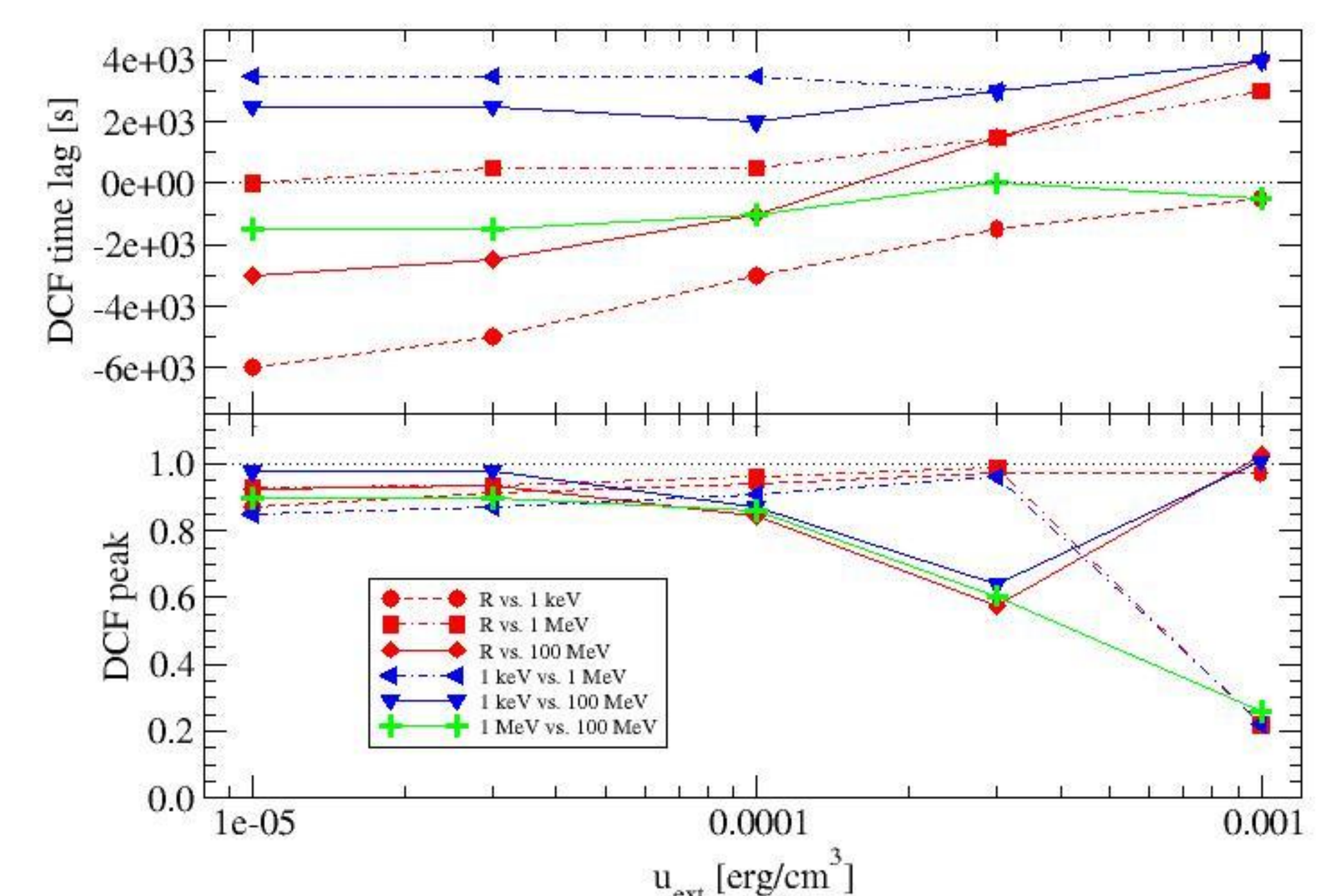


Fig. 5: Dependence on DCF parameters on the external radiation energy density.

With current observational capabilities, our results may be compared to cross correlations of observations of FSRQs and LBLs by ground-based optical observatories and pointing X-ray telescopes, while the required time resolution at gamma-ray energies is currently beyond the capabilities of INTEGRAL (soft γ -rays) and Fermi and AGILE (HE γ -rays).